



available at www.sciencedirect.com



journal homepage: www.elsevier.com/locate/fsi



# Molecular modelling of co-receptor CD8 $\alpha\alpha$ and its complex with MHC class I and T-cell receptor in sea bream (*Sparus aurata*)

Susan Costantini <sup>a</sup>, Francesco Buonocore <sup>b</sup>, Angelo M. Facchiano <sup>a,\*</sup>

<sup>a</sup> *Laboratorio di Bioinformatica e Biologia Computazionale, Istituto di Scienze dell'Alimentazione – CNR, via Roma 52 A/C, 83100 Avellino, Italy*

<sup>b</sup> *Dipartimento di Scienze Ambientali, University of Tuscia, Largo dell'Università, 01100 Viterbo, Italy*

Received 9 January 2008; revised 19 March 2008; accepted 30 March 2008

## KEYWORDS

*Sparus aurata*;  
Molecular modelling;  
Protein structure;  
CD8;  
T-cell receptor;  
MHC-I

**Abstract** T-cells are the main actors of cell-mediated immune defence; they recognize and respond to peptide antigens associated with MHC class I and class II molecules. In this paper, we investigated by molecular modelling methods in the teleost sea bream (*Sparus aurata*) the interaction among the molecules of the tertiary complex CD8/MHC-I/TCR, which determines the T-cell-mediated immunological response to foreign molecules. First, we predicted the three-dimensional structure of CD8 $\alpha\alpha$  dimer and MHC-I, and, successively, we simulated the CD8 $\alpha\alpha$ /MHC-I complex. Finally, the 3D structure of the CD8/MHC-I/TCR complex was simulated in order to investigate the possible changes that can influence TCR signalling events.

© 2008 Published by Elsevier Ltd.

## Introduction

T-cell-mediated immunity is one of the main lines of defence that vertebrates rely on for eliminating microbial pathogens. While antibodies recognize intact antigens, T-cells distinguish foreign material from self through presentation of fragments of the antigen by the MHC cell surface receptors. Only if an MHC molecule presents a specific antigenic peptide will a cellular immune response be triggered. The recognition and signalling events require

the activities of several T-cell receptor (TCR) associated molecules, including co-receptors CD3, CD8 or CD4, and other costimulatory receptors [1].

In the cellular immune response, the antigens, generally peptides, are displayed to T-cells in complex with class I or class II MHC molecules. The peptide binding site is constituted by  $\alpha 1$ - $\alpha 2$  domains of MHC-I molecules and  $\alpha 1$ - $\beta 1$  domains of MHC-II molecules. These molecules present the peptides to TCR in an extended conformation via a vice-like groove, comprising two  $\alpha$ -helices and a floor composed of anti-parallel  $\beta$ -strands [2–5]. T-cell receptors are cell surface heterodimers consisting of either disulphide-linked  $\alpha$ - and  $\beta$ - or  $\gamma$ - and  $\delta$ -chains. Each TCR chain is composed of a variable and a constant Ig-like domain, followed by a transmembrane domain and a short cytoplasmic tail [2,3].

\* Corresponding author. Tel.: +39 0825 299625; fax: +39 0825 781585.

E-mail address: [angelo.facchiano@isa.cnr.it](mailto:angelo.facchiano@isa.cnr.it) (A.M. Facchiano).

The  $\alpha\beta$  TCRs bind MHC through complementary-determining regions (CDR loops) present in variable domains and are oriented approximately diagonally relative to the long axis of the MHC peptide-binding groove [6,7]. The co-receptors CD8 and CD4 stabilize the interaction of the T-cell receptor with MHC-I [8]. In particular, CD8 molecules are expressed as homo- or heterodimers and both chains are composed of an extracellular Ig Vdomain, a membrane-proximal hinge region, a transmembrane domain and a cytoplasmic tail [9] responsible for interaction with a lymphocyte specific kinase (p56lck) [10–12]. CD8 exerts its activity of TCR co-receptor by interacting with MHC-I and  $\beta_2$ -microglobulin ( $\beta_2$ -m) during TCR-mediated MHC recognition [4,13,14]. Structural studies have shown that CD8 $\alpha\alpha$  associates with  $\beta_2$ -m and the  $\alpha 2$  and  $\alpha 3$  domains of MHC using the A and B strands and CDR loops within its V domain. Protein crystallographic studies on human or mouse molecules have investigated the interactions in these binary complexes but no complete system complex, i.e. CD8 $\alpha\alpha$ /MHC-I/TCR $\beta$ , has been yet experimentally characterized.

In teleost fishes CD8, MHC-I and TCR molecules have been recently evidenced. In particular, in sea bream (*Sparus aurata*) the CD8 $\alpha$  [8], MHC-I  $\alpha$  [15], MHC-II  $\alpha$  [16] and TCR  $\beta$  [17] genes have been cloned. This gives us the possibility to investigate by molecular modelling the 3D structure of CD8 $\alpha\alpha$ , MHC-I and the complexes formed by CD8 $\alpha\alpha$ /MHC-I and CD8 $\alpha\alpha$ /MHC-I/TCR. The interaction among the molecules in the complexes has been analysed in order to study the molecular basis that influences recognition and signalling events.

## Methods

### Modelling of sea bream CD8 $\alpha\alpha$ homodimer

The three-dimensional model of two sea bream CD8 $\alpha 1$  and CD8 $\alpha 2$  (EMBL entry: AJ878605.3) chains (see Results and Discussion for motivation) was performed according to the comparative modelling strategy using the template structures of human and murine CD8 $\alpha 1$  (PDB code: 1AKJ, chain D, and 1BQH, chain H) and CD8 $\alpha 2$  (PDB code: 1AKJ, chain E, and 1BQH, chain G), respectively [4,5].

As the sequence identities between the sea bream chains and the homologous template models were lower than 30%, we used a procedure, already applied and described in previous similar works [17–22], to search for the best alignment of sequences. In detail, the multiple alignment of many CD8 sequences was made and few manual refinements were added to account for the position of secondary structures. This protocol allows us to improve the alignment of the template and target protein sequences, as well as to avoid the presence of gaps and insertions in secondary structure elements, which are often responsible for wrong models.

The MODELLERv7 module [23] implemented in Insight II program (Accelrys, San Diego, CA) was used to build 10 full-atom models of both CD8 $\alpha 1$  and CD8 $\alpha 2$  chains by setting 4.0 Å as root mean square deviation (RMSD) among initial models and by full model optimization. To select the best models, we used the ProSall program [24] to check the fitness of the sequences relative to the obtained

structures and to assign a scoring function, and the PRO-CHECK program [25] to evaluate their stereochemical and structural packing quality. Secondary structures were assigned by the DSSP program [26]. Search for structural classification was performed on the CATH database [27,28].

The structure of sea bream CD8 $\alpha\alpha$  dimer was assembled by superimposing the two best modelled chains of sea bream CD8 $\alpha 1$  and CD8 $\alpha 2$  to the corresponding murine CD8 chains, in order to obtain the same relative orientation of the two subunits. The CVFF force field within the Discover module of Insight II was used to assign potentials and charges, and a mild energy minimization was applied, by performing 500 steps under the conjugate gradient algorithm, in order to optimise the interaction between the two sea bream protein chains and avoid sterical clashes according to the procedure used in our previous similar work [29].

### 3D modelling of sea bream MHC-I

The modelling of sea bream MHC-I N-terminal region (20–200 amino acid region, accession number: DQ211541.1) was performed using as template the human and murine experimental structures of MHC-I complexed with TCR  $\beta$  (PDB code: 2GJ6, chain A, and 1G6R, chain H) [2,3]. The modelling of the C-terminal region (201–295 amino acid region, accession number: DQ211541.1) was instead based on the experimental human and murine structures of MHC-I complexed with CD8 $\alpha\alpha$  (PDB code: 1AKJ chain A, and 1BQH chain A) [4,5]. The sequence identity percentages between sea bream MHC-I and man/mouse resulted in 31% and 34%, respectively. The 3D structure of sea bream MHC-I was modelled and analysed with the same procedures and software described above for CD8.

### Simulation of sea bream CD8 $\alpha\alpha$ /MHC-I and CD8 $\alpha\alpha$ /MHC-I/V $\beta$ complexes

The sea bream CD8 $\alpha\alpha$ /MHC-I and CD8 $\alpha\alpha$ /MHC-I/V $\beta$  complexes were created starting from the reference experimental models of murine CD8 $\alpha\alpha$ /MHC-I [5] and V $\beta$ /MHC-I [4], respectively. In detail, we created the sea bream CD8 $\alpha\alpha$ /MHC-I and V $\beta$ /MHC-I complexes by superimposing the sea bream coordinates on those of murine corresponding molecules in the two available experimental complexes. For the V $\beta$  (i.e. TCR variable beta) region of the sea bream T-cell receptor (21–240 region, accession number: AM490437) we used the three-dimensional model already described in our recent paper [17]. Moreover, to simulate the sea bream CD8 $\alpha\alpha$ /MHC-I/V $\beta$  complex we superimposed the identical MHC-I chains present in the two sea bream CD8 $\alpha\alpha$ /MHC-I and V $\beta$ /MHC-I complexes. The complexes were minimized using the same procedure described in previous similar works [15,19,29–32]. To compare the protein-protein interaction in the complexes, the “Protein-Protein Interaction Server” [33] and the program NACCESS [34] were used to evaluate the interface surface area and to identify the amino acids at the protein-receptor interface. H-bonds were calculated with the Hbplus program [35]. Moreover, the binding free energy between the different chains was calculated by using the DCOMPLEX program [36].





## Results and discussion

### Modelling of sea bream CD8 $\alpha\alpha$ dimer

The sequence of sea bream CD8 $\alpha$  resulted similar to 20 protein sequences, defined as "CD8", from different organisms. The e-values computed by means of the BLAST software resulted in all  $<10e^{-6}$  and this confirms a significant similarity of these sequences with sea bream CD8 $\alpha$ .

The percentage of sequence identity between CD8 in sea bream and the other sequences ranged from 59% to 36% for teleost fish sequences, and from 33% to 26% for mammal sequences. In Fig. 1, we show the alignment of human, mouse, sea bream and other six fish sequences. Human and mouse sequences are of particular interest in our study because the three-dimensional structure of these proteins has been experimentally solved. On the basis of this knowledge, it is possible to build a theoretical model for the homologous protein from sea bream, by applying the homology modelling strategy or comparative modelling. The reliability of the theoretical models obtained by this strategy is considered very high, but it requires a careful application of a number of software and validation tools as described in the Materials and Methods section. In this case, the experimental three-dimensional structures of human and murine CD8 $\alpha_1$  (PDB code: 1AKJ, chain D, and 1BQH, chain H) and CD8 $\alpha_2$  (PDB code: 1AKJ, chain E, and 1BQH, chain G) have been used for comparative modelling of sea bream CD8 $\alpha_1$  and CD8 $\alpha_2$ . We constructed two CD8 models because these two chains have an identical sequence but may show some conformational differences as reported for experimental murine and human structures. Starting from the alignment of the CD8 sequences (Fig. 1), we created 10 structural models for the 22–128 region of two sea bream CD8 $\alpha$  chains and selected the best models on the basis of stereochemical and energy parameters (see Methods). Both models present 10 beta-strands (ABCC'C'D'EFGH), involving about 50% of the sequence and define the global structure as an immunoglobulin-like beta-sandwich made of two anti-parallel sheets. Three loop regions are present between B and C strands (CDR1), between C' and C'' strands (CDR2) and between F and G strands (CDR3). The two cysteines present in B and F strands (Cys 17-Cys85) are at a suitable distance to form an S-S bond (see Fig. 2), as happens in the template human and mouse structures [4,5]. These cysteines are conserved in all CD8 sequences from teleost fishes as reported in a recent paper [15]. Moreover, the sea bream CD8 $\alpha_1$  and CD8 $\alpha_2$  models were compared by structural superimposition obtaining an RMSD value of 0.85 Å. The comparison of secondary structures shows that all  $\beta$ -strands are quite conserved with some little differences. These evaluations suggest that these two chains have a similar tertiary structure and the differences are located at the level of CDR loops.

The CD8 $\alpha\alpha$  dimer was analysed in terms of interaction residues and interchain H-bond number. The two sea bream CD8 $\alpha$  chains form a dimer that has pseudodyad symmetry according to human and murine dimers. In the CD8 $\alpha\alpha$  dimer one hydrogen bond is formed among Glu115 of CD8 $\alpha_1$  and Thr74 of CD8 $\alpha_2$  and the interface is constituted by 17 and 19 amino acids of CD8 $\alpha_1$  and CD8 $\alpha_2$ , respectively. In detail,

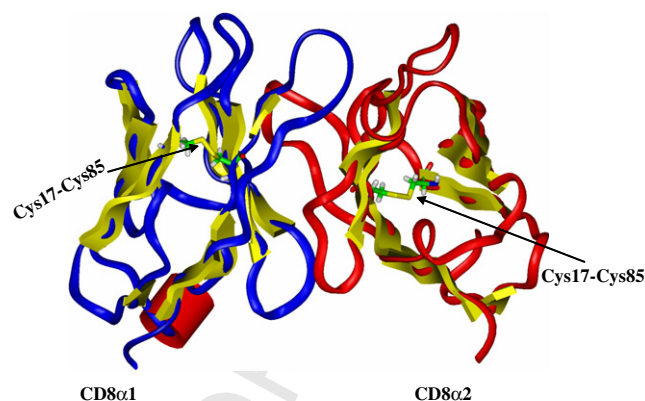


**Figure 2** 3D model of sea bream CD8 $\alpha\alpha$  dimer. The backbone ribbon is reported in blue for CD8 $\alpha_1$  and in red for CD8 $\alpha_2$ .  $\beta$ -strands are indicated with yellow arrows and helices with red cylinders. Green and yellow sticks indicate the presence of two putative intrachain disulphide bonds.

the dimer interaction in sea bream CD8 $\alpha\alpha$  is mediated by the CDR3-like domain, the C-C' loop and the G and C' strands as in the human and mouse [37]. Both the G and C' strands of this immunoglobulin-like domain contain highly conserved beta-bulges that are found at the dimer interface and are believed to play an important role in facilitating dimerization [38,39]. The conserved sequence motifs for the C' strand bulge (i.e. ProThrPheLeuLeu and ValVal in human and mouse CD8 $\alpha\alpha$ , respectively), and for the G strand bulge (i.e. PheSerHisPhe and SerSer in human and mouse CD8 $\alpha\alpha$ , respectively) are not conserved in sea bream. Moreover, the sea bream CD8 $\alpha\alpha$  homodimer burying aromatic residues, i.e. Trp50, Tyr105 and Tyr111, in the dimer interface shares, as expected, the same dimerization features of human and murine CD8 $\alpha\alpha$  [4,5].

### 3D modelling of sea bream MHC-I

The 3D MHC-I model (Fig. 3) in sea bream has a classical organization in three distinct domains. Two G- $\alpha_1$  [D1] and G- $\alpha_2$  [D2] domains are classified as "alpha-beta" and each consists of an alpha helical region and four strands of beta sheets in an anti-parallel orientation. The third domain (C-like [D3]) has a "mainly beta" fold and is characterized by an immunoglobulin-like beta-sandwich made of two anti-parallel sheets, each consisting of three main strands and few shorter strands, organized in greek-key motifs. In the sea bream MHC-I model four cysteine residues are located in the same positions of the human and murine templates and they should form two intrachain disulfide bonds in the second and third domains, respectively. The sea bream MHC-I model was compared by structural superimposition with the experimental structures used as templates even if the presence of gaps in the alignment made it difficult to perform a complete structural comparison of the three models. RMSD values obtained comparing the N-terminal regions of human/murine templates complexed with V $\beta$  and sea bream MHC-I model resulted in 0.79 and 0.63 Å respectively, whether those obtained for the C-terminal regions of human/murine

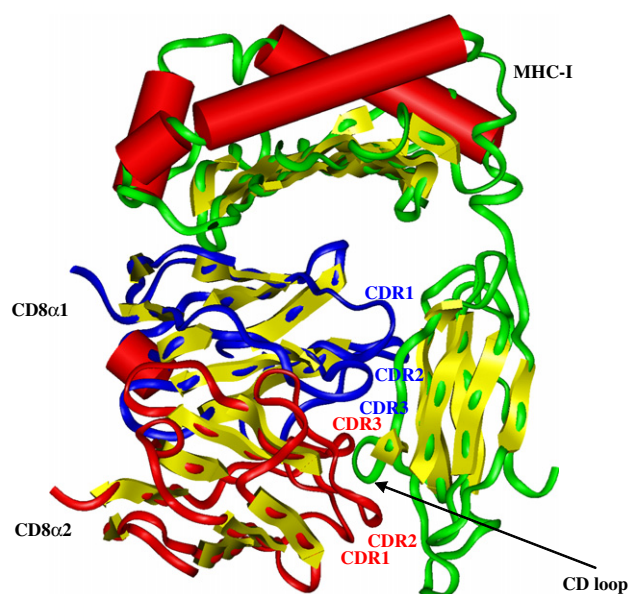


**Figure 3** 3D model of sea bream MHC-I/CD8 $\alpha\alpha$  complex. The backbone ribbon is reported in green for MHC-I, in blue for CD8 $\alpha$ 1 and in red for CD8 $\alpha$ 2. Secondary structure topology is shown: yellow arrows represent  $\beta$ -strands and red cylinders represent  $\alpha$ -helices. Green and yellow sticks indicate the presence of disulphide bonds. The labels indicate the CD loop in MHC-I and three CDR-like loops in the CD8 $\alpha\alpha$  dimer.

**Table 1** Analysis of the three complexes in terms of interface surface area ( $\text{\AA}^2$ ), interchain H-bonds and number of interaction residues

	Interface surface area ( $\text{\AA}^2$ )	Interchain H-bonds	Interaction residues
<i>MHC-I/CD8<math>\alpha\alpha</math> complex</i>			
MHC-I	605.86	6	22
CD8 $\alpha$ 1	645.08	6	18
MHC-I	665.78	9	18
CD8 $\alpha$ 2	654.95	9	18
<i>MHC-I/CD8<math>\alpha\alpha</math>/V<math>\beta</math> complex</i>			
MHC-I	609.98	6	18
CD8 $\alpha$ 1	652.80	6	16
MHC-I	686.43	9	16
CD8 $\alpha$ 2	684.24	9	14
MHC-I	634.81	7	17
V $\beta$	657.61	7	19
<i>MHC-I/V<math>\beta</math> complex</i>			
MHC-I	622.88	4	18
V $\beta$	640.17	4	18

templates complexed with CD8 and our sea bream model resulted in 0.58 and 0.75  $\text{\AA}$ , respectively. These values indicated that our model keeps the typical architecture of MHC-I in agreement with the structural classification

**Table 2** The list of interaction residues between MHC-I, CD8 $\alpha\alpha$  and V $\beta$  in the three complexes

MHC-I/CD8 $\alpha\alpha$ complex	Interaction residues
MHC-I	N110,Q114,D121,D126,L127,I133,A134,P135,H208 R209,A210,S211,V213,E220,H222,V225,H227,G228 E229,F230,M240,Q261
CD8 $\alpha$ 1	E24,V25,K37,H40,P43,G44,S45,M46,I48,S65 S66,N67,Q88,L110,Y111,K112,G113,L116
MHC-I	T193,P194,S195,S196,V213,V214,E219,E220,L221 H222,E223,E224,V225,D226,H227,K245,L246,S247
CD8 $\alpha$ 2	P43,G44,S45,M46,I47,I48,F60,S65,S66,N67,M69 P70,K85,T109,L110,Y111,K112,G113
<i>MHC-I/CD8<math>\alpha\alpha</math>/V<math>\beta</math> complex</i>	
MHC-I	Q114,L127,I133,P135,H208,R209,A210,S211,V213 E220,H222,V225,H227,G228,E229,F230,M240,Q261
CD8 $\alpha$ 1	E24,K37,H40,P43,G44,S45,M46,I48,S65 S66,N67,Q88,L110,Y111,K112,G113
MHC-I	P194,S195,S196,V213,V214,E219,E220,L221 H222,E223,E224,V225,D226,H227,K245,L246
CD8 $\alpha$ 2	P43,G44,S45,M46,S65,S66,N67,P70,K85 T109,L110,Y111,K112,G113
MHC-I	G69,Q72,T73,K75,A76,D79,Q83,I141,K145,W146 D147,N148,N149,K150,G151,L152,L155
V $\beta$	K46,T48,S49,Y50,Y51,E52,T71,Q72,S73,P74,P75 Q77,E79,K92,D93,A94,G119,E120,Y101,E122
<i>MHC-I/V<math>\beta</math> complex</i>	
MHC-I	G69,Q72,T73,K75,A76,I78,D79,Q83,I141,K145 W146,D147,N148,N149,K150,G151,L152,L155
V $\beta$	K46,T48,S49,Y50,Y51,E52,T71,Q72,S73,P74 P75,Q77,E79,A94,G119,N120,T121,H124

reported by the CATH database [27,28] for the crystallographic structures of human and murine MHC-I molecules. Moreover, the comparison of the secondary structures evidenced that helices and beta-strands are well conserved along the sequence, with just some residue which may increase or decrease their length.

### Simulation of sea bream CD8aa/MHC-I complex

On the basis of the crystallographic structure of the murine CD8 $\alpha$ /MHC-I complex we simulated the interaction between CD8 $\alpha$  and MHC-I in sea bream (Fig. 3). For this complex, we evaluated the interaction residues, the

number of interchain H-bonds and the interface surface area (Tables 1 and 2). MHC-I and CD8 $\alpha$ 1 chains may form six H-bonds at their surface of interaction, while MHC-I and CD8 $\alpha$ 2 nine H-bonds. The interaction regions between MHC-I and CD8 $\alpha$ 1/CD8 $\alpha$ 2 in mammalian and sea bream complexes are well conserved (Fig. 4) even if only few amino acids are conserved between fish and mammalian molecules. The CD8 $\alpha$ 1 and CD8 $\alpha$ 2 subunits make interactions through their CDR-like loops (CDR1, CDR2 and CDR3) with the  $\alpha$ 3 domain (C-like [D3]) of MHC-I. Moreover, CD8 $\alpha$ 1 interacts also with the  $\alpha$ 2 domain (G- $\alpha$ 2 [D2]) of MHC-I. The major contribution of MHC-I  $\alpha$ 3 is provided from the protruding loop region (Glu220-Asp226) interacting with

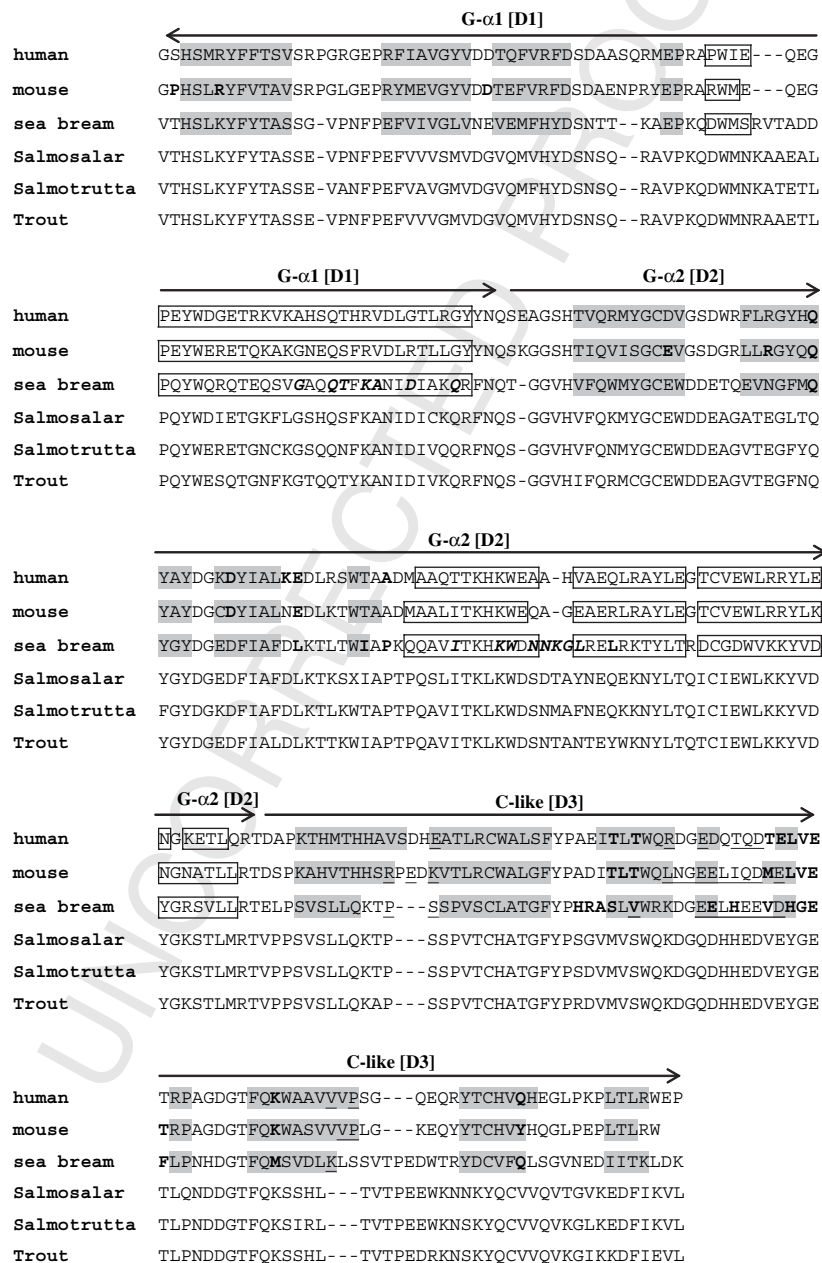


**Figure 4** Alignment of MHC-I in human, mouse, sea bream, *Salmosalar*, *Salmotrutta* and trout. Amino acids in beta-strands are evidenced in grey but those in the helix are reported in a box. Amino acids in bold interact with CD8 $\alpha$ 1 and those underlined with CD8 $\alpha$ 2. The residues at the interface with V $\beta$  are reported in italics and bold. The labels indicate the different structural domains.



745 the CD8 $\alpha$  subunits by main chain and side chain interactions  
 746 according to experimental complexes [40,41]. In detail, this  
 747 relatively rigid loop (indicated as loop CD) protrudes into  
 748 the antigen-binding-like pocket formed by the six CDR-  
 749 like loops of the CD8 $\alpha\alpha$  homodimer. A second distinctive  
 750 feature essential for the interaction between MHC-I and  
 751 CD8 $\alpha\alpha$  is the AB loop of the MHC  $\alpha$ 3 domain, which  
 752 interacts with the CDR2-loop of CD8 $\alpha$ 2. A third aspect  
 753 that is characteristic of sea bream MHC-I/CD8 $\alpha\alpha$  complex  
 754 regards the interaction between the MHC  $\alpha$ 3 domain and  
 755 the N-terminal residues of the CD8 $\alpha$ 1 subunit.

756 Moreover, the comparison of the specific interaction  
 757 residues found in sea bream MHC-I with respect to other fish  
 758 species shows that 35% of the amino acids are conserved as  
 759 reported in Fig. 4. In the case of CD8 $\alpha$  molecules we can  
 760 note that some structural interactions are in common  
 761 only within sea bream and sea bass.

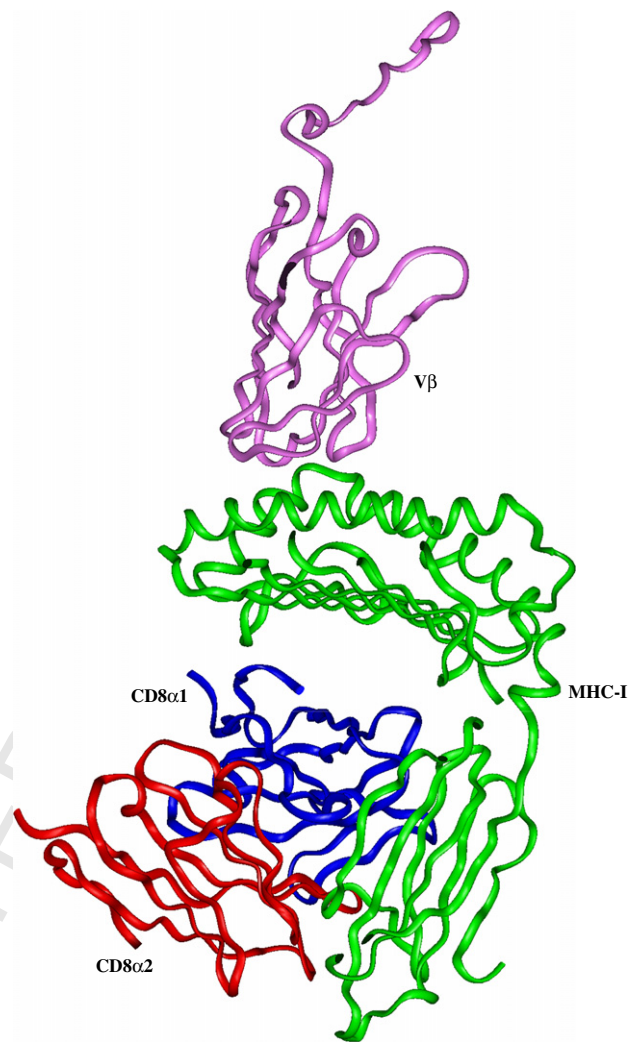
762 There is no significant change in the CD8 $\alpha\alpha$  homodimer  
 763 structure between the un-complexed versus MHC-I bound  
 764 state as for human and mouse [4,5]. Finally, it is important  
 765 to underline that  $\beta$ 2-m interacts with MHC-I and CD8 $\alpha$ 1  
 766 [13,14] and will influence the interaction between these  
 767 two chains in the complex. However, the sequence of sea  
 768 bream  $\beta$ 2-m is still unknown, and for this reason we simu-  
 769 lated only the interaction between MHC-I and CD8 $\alpha\alpha$ .  
 770 Similarly, the presence of the antigenic peptide in the  
 771 MHC groove would be useful to simulate the conformation  
 772 of the MHC molecule when it binds the peptide. Unfortu-  
 773 nately, there is no information about the sequence of an  
 774 antigenic peptide which interacts with MHC class I in sea  
 775 bream.

### 776 Simulation of sea bream CD8 $\alpha\alpha$ /MHC-I/V $\beta$ complex

777 The crystallographic studies on  $\alpha\beta$  T-cell receptors bound to  
 778 MHC-I or MHC-II or to TR co-receptors (CD4 and CD8) have  
 779 further advanced our knowledge on structural variability  
 780 of TR/MHC recognition and on the amino acid segments  
 781 that constitute the TR signalling complex. Despite all these  
 782 efforts, the structural basis for MHC restriction and signal-  
 783 ling remains elusive and no structural features that define  
 784 a common binding mode or signalling mechanism have yet  
 785 been determined. In fact, in the absence of a ternary  
 786 CD8/MHC-I/V $\beta$  complex structure, no conclusions can yet  
 787 be drawn to the precise role that the V $\beta$ /MHC docking  
 788 geometry plays in co-receptor binding and downstream  
 789 signalling [1].

792 For these reasons, we created a model for CD8 $\alpha\alpha$  and V $\beta$   
 793 bound to MHC class I (see Fig. 5). The sea bream V $\alpha$   
 794 sequence was not included in the complex because it is still  
 795 unknown. Certainly its absence could influence the struc-  
 796 ture of V $\beta$ /MHC-I complex. However, we modelled the sea  
 797 bream V $\beta$  using as template the mammalian V $\beta$  structure  
 798 already complexed with the V $\alpha$  chain and this gave us the  
 799 possibility to take into account the V $\beta$  influence on the  
 800 complex [31]. In fact, using this procedure it is possible  
 801 to simulate the conformational changes occurring when  
 802 a protein interacts with its receptor.

803 The binding sites of CD8 $\alpha\alpha$  and V $\beta$  to MHC-I are spatially  
 804 separated even if it is known that they require similar ori-  
 805 entations with respect to the MHC  $\alpha$ 3 domain [1]. In detail,  
 806 the amino acids of MHC-I at the interface with V $\beta$  chain are



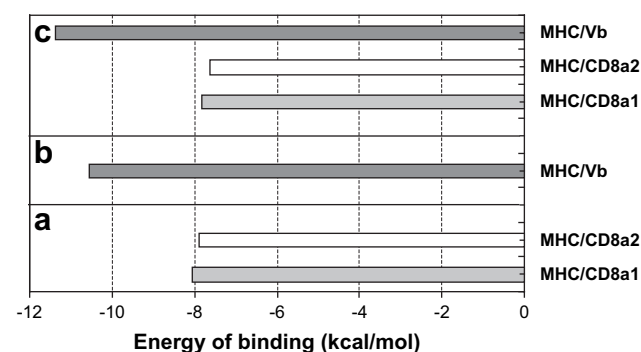
807  
808  
809  
810  
811  
812  
813  
814  
815  
816  
817  
818  
819  
820  
821  
822  
823  
824  
825  
826  
827  
828  
829  
830  
831  
832  
833  
834  
835  
836  
837  
838  
839  
840  
841  
842  
843  
844  
845  
846  
847  
848  
849  
850  
851  
852  
853  
854  
855  
856  
857  
858  
859  
860  
861  
862  
863  
864  
865  
866  
867  
868

Figure 5 3D model of sea bream MHC-I/CD8 $\alpha\alpha$ /V $\beta$  complex. The backbone ribbon is reported in green for MHC-I, in blue for CD8 $\alpha$ 1, in red for CD8 $\alpha$ 2 and in pink for V $\beta$ .

located mainly in helical regions comprised in G- $\alpha$ 1 [D1] and G- $\alpha$ 2 [D2] domains and those at the interface with CD8 $\alpha\alpha$  are located in loop and beta regions located in G- $\alpha$ 2 [D2] and C-like [D3] domains (see Fig. 4).

We compared the two sea bream complexes simulated in this work (i.e. CD8 $\alpha\alpha$ /MHC-I, and CD8 $\alpha\alpha$ /MHC-I/V $\beta$ ) and the MHC-I/V $\beta$  recently published [17] in terms of interaction residues, number of interchain H-bonds and interface surface area (Tables 1 and 2). These complexes show little differences in the interface surface area values and number of interaction residues.

The number of interchain H-bonds between MHC-I and CD8 $\alpha\alpha$  is the same in both CD8 $\alpha\alpha$ /MHC-I and CD8 $\alpha\alpha$ /MHC-I/V $\beta$  complexes but taking into consideration MHC-I and V $\beta$  this number is higher in the CD8 $\alpha\alpha$ /MHC-I/V $\beta$  complex with respect to MHC-I/V $\beta$  (see Table 1). Moreover, for each complex we have evaluated the binding energy (Fig. 6) between the different chains. The binding energy between MHC-I and CD8 $\alpha\alpha$  is similar in CD8 $\alpha\alpha$ /MHC-I and CD8 $\alpha\alpha$ /MHC-I/V $\beta$  complexes with a difference of only 0.2 kcal/mol, whether this value between MHC-I and V $\beta$  is higher



**Figure 6** Binding free energies for the complexes. The bars represent the binding energies (expressed in kcal/mol) evaluated for MHC/CD8 $\alpha\alpha$  (panel a), MHC/V $\beta$  (panel b) and MHC/CD8 $\alpha\alpha$ /V $\beta$  (panel c) complexes.

(of about 0.8 kcal/mol) in the CD8 $\alpha\alpha$ /MHC-I/V $\beta$  compared Q8 to MHC-I/TR $\beta$ .

These results suggest that the binding of sea bream CD8 $\alpha\alpha$  to MHC-I should increase the affinity of V $\beta$  for MHC-I and stabilize the MHC-I/V $\beta$  complex. Therefore, the observation that the binding sites of CD8 and TR to MHC-I are spatially distinct but require similar orientations of the MHC  $\alpha$ 3-domain, is consistent with an avidity-based contribution of the CD8 to the MHC-I-TR binding, as already reported [4].

## Conclusions

Despite the impressive increase in the cloning and expression of genes coding in fish for immunoregulatory molecules, the knowledge on “in vivo” and “in vitro” functional immunology of corresponding peptide products is still at the beginning. Structural studies could help in improving our Q9 knowledge on the behaviour of these molecules until specific markers for immunoregulatory peptides will be available. Moreover, it may be possible to design some peptides, based on the amino acids present at the interface of the modelled complexes, that can block complex formation and that, therefore, should inhibit T-cell activation in vitro and permit interesting functional analyses, as already performed in mammals [42].

## Acknowledgements

This work was partially supported by the CNR-Bioinformatics Project and by the European Commission within the project IMAQUANIM (EC contract number FOOD-CT-2005-007103).

## References

- [1] Rudolph MG, Stanfield RL, Wilson IA. How TCRs bind MHCs, peptides and coreceptors. *Annu Rev Immunol* 2006;24:419–66.
- [2] Gagnon SJ, Borbulevich OY, Davis-Harrison RL, Turner RV, Damirjian M, Wojnarowicz A, et al. T cell receptor recognition via cooperative conformational plasticity. *J Mol Biol* 2006;363:228–43.
- [3] Degano M, Garcia KC, Apostolopoulos V, Rudolph MG, Teyton L, Wilson IA. A functional hot spot for antigen

recognition in a superagonist TCR/MHC complex. *Immunity* 2000;12:251–61.

- [4] Gao GF, Tormo J, Gerth UC, Wyer JR, McMichael AJ, Stuart DI, et al. Crystal structure of the complex between human CD8 $\alpha$ -phosphatase and HLA-A2. *Nature* 1997;387(6633):630–4.
- [5] Kern PS, Teng MK, Smolyar A, Liu JH, Liu J, Hussey RE, et al. Structural basis of CD8 coreceptor function revealed by crystallographic analysis of a murine CD8 $\alpha$ phosphatase ectodomain fragment in complex with H-2Kb. *Immunity* 1998;9(4):519–30.
- [6] Garcia KC, Degano M, Stanfield RL, Brunmark A, Jackson MR, Peterson PA, et al. An  $\alpha\beta$  T cell receptor structure at 2.5 Angstroms and its orientation in the TCR–MHC complex. *Science* 1996;274:209–19.
- [7] Garboczi DN, Ghosh P, Utz U, Fan QR, Biddison WE, Wiley DC. Structure of the complex between human T-cell receptor, viral peptide and HLA-A2. *Nature* 1996;384:134–41.
- [8] Randelli E, Foglietta A, Mazzini M, Scapigliati G, Buonocore F. Cloning and expression analysis of the co-receptor CD8 $\alpha$  in sea bream (*Sparus aurata* L.). *Aquaculture* 2006;256:631–7.
- [9] Frazer JK, Capre JD. Structure and function of immunoglobulin. *Fundam Immunol* 1999;4:37–74.
- [10] Veillette A, Bookman MA, Korak EM, Bolen JB. The CD4 and Cd8 T cell surface antigens are associated with the internal membrane tyrosine-protein kinase p56lck. *Cell* 1988;55:301–8.
- [11] Veillette A, Horak ID, Korak EM, Bookman MA, Bolen JB. Alteration of the lymphocyte-specific protein tyrosine kinase (p56lck) during T-cell activation. *Mol Cell Biol* 1988b;8:4353–61.
- [12] Letourner F, Gabert J, Cosson P, Blanc D, Davoust J, Malissen B. A signalling role for the cytoplasmic segment of the CD8 alpha chain detected under limiting stimulatory conditions. *Proc Natl Acad Sci USA* 1990;87:2339–43.
- [13] Salter RD, Benjamin RJ, Wesley PK, Buxton SE, Garrett TP, Clayberger C, et al. A binding site for the T-cell co-receptor CD8 on the alpha3 domain of HLA-A2. *Nature* 1990;345:41–6.
- [14] Sanders SK, Fox RO, Kavathas P. Mutations in CD8 that affect interactions with HLA class I and monoclonal anti-CD8 antibodies. *J Exp Med* 1991;174:371–9.
- [15] Cuesta A, Meseguer J, Esteban MA. Cloning and regulation of the major histocompatibility class I alpha gene in the teleost fish gilthead seabream. *Fish Shellfish Immunol* 2007;22(6):718–26.
- [16] Cuesta A, Esteban MA, Meseguer J. Cloning, distribution and up-regulation of the teleost fish MHC class II alpha suggests a role for granulocytes as antigen-presenting cells. *Mol Immunol* 2006;43(8):1275–85.
- [17] Randelli E, Scala V, Casani D, Costantini S, Facchiano A, Mazzini M, et al. T cell receptor beta chain from sea bream (*Sparus Aurata*): molecular cloning, expression and modelling of the complexes with MHC class I. *Mol Immunol* 2008;45:2017–27.
- [18] Facchiano AM, Stiuso P, Chiusano ML, Caraglia M, Giuberti G, Marra M, et al. Homology modelling of the human eukaryotic initiation factor 5A (eIF-5A). *Protein Eng* 2001;14:881–90.
- [19] Scapigliati G, Costantini S, Colonna G, Facchiano A, Buonocore F, Bossù P, et al. Modelling of fish interleukin 1 and its receptor. *Dev Comp Immunol* 2004;28:429–41.
- [20] Buonocore F, Randelli E, Bird S, Secombes CJ, Costantini S, Facchiano A, et al. The CD8 $\alpha$  from sea bass (*Dicentrarchus labrax* L.): cloning, expression and 3D modelling. *Fish Shellfish Immunol* 2006;20:637–46.
- [21] Buonocore F, Randelli E, Casani D, Costantini S, Facchiano A, Scapigliati G, et al. Molecular cloning, differential expression and 3D structural analysis of the MHC class-II beta chain from sea bass (*Dicentrarchus labrax* L.). *Fish Shellfish Immunol* 2007;23:853–66.
- [22] Buonocore F, Randelli E, Bird S, Secombes CJ, Facchiano A, Costantini S, et al. Interleukin-10 expression by real-time



- 993 PCR and homology modelling analysis in the European sea  
994 bass (*Dicentrarchus Labrax* L.). *Aquaculture* 2007;270:  
995 512–22.
- [23] Sali A, Blundell TL. Comparative protein modelling by satisfac-  
996 tion of spatial restraints. *J Mol Biol* 1993;234:779–815. 1027
- [24] Sippl MJ. Recognition of errors in three-dimensional structures  
997 of proteins. *Proteins* 1993;17:355–62. 1028
- [25] Laskowski RA, MacArthur MW, Moss DS, Thornton JM. PRO-  
1000 CHECK – A program to check the stereochemical quality of  
1001 protein structures. *J Appl Cryst* 1993;26:283–91. 1029
- [26] Kabsch W, Sander C. Dictionary of protein secondary  
1002 structure: pattern recognition of hydrogen-bonded and  
1003 geometrical features. *Biopolymers* 1983;22:2577–637. 1030
- [27] Orengo CA, Michie AD, Jones S, Jones DT, Swindells MB,  
1004 Thornton JM. CATH – a hierarchic classification of protein  
1005 domain structures. *Structure* 1997;5:1093–108. 1031
- [28] Pearl FMG, Lee D, Bray JE, Sillitoe I, Todd AE, Harrison AP,  
1006 et al. Assigning genomic sequences to CATH. *Nucleic Acids*  
1007 *Res* 2000;28:277–82. 1032
- [29] Costantini S, Colonna G, Rossi M, Facchiano AM. Modelling of  
1008 HLA-DQ2 and simulations of its interaction with gluten  
1009 peptides to explain molecular recognition in celiac disease.  
1010 *J Mol Graph Model* 2005;23:419–31. 1033
- [30] Chambery A, Pisante M, Di Maro A, Di Zazzo E, Costantini S,  
1011 Colonna G, et al. Invariant Ser211 is involved in the catalysis  
1012 of PD-L4, type I RIP from (*Phytolacca dioica*) leaves. *Proteins:*  
1013 *Struct Func Bioinform* 2007;67:209–18. 1034
- [31] Costantini S, Colonna G, Facchiano AM. Simulation of confor-  
1014 mational changes occurring when a protein interacts with its  
1015 receptor. *Comput Biol Chem* 2007;31(3):196–206. 1035
- [32] Gianfrani C, Siciliano R, Facchiano AM, Camarca A,  
1016 Mazzeo FM, Costantini S, et al. Transamidation of wheat flour  
1017 inhibits the response to gliadin of intestinal T cells in celiac  
1018 disease. *Gastroenterology* 2007;133:780–9. 1036
- [33] Jones S, Thornton JM. Principles of protein–protein interac-  
1019 tions derived from structural studies. *Proc Natl Acad Sci USA*  
1996;93:13–20. 1037
- [34] Hubbard SJ, Campbell SF, Thornton JM. Molecular recognition.  
1020 Conformational analysis of limited proteolytic sites and serine  
1021 proteinase protein inhibitors. *J Mol Biol* 1991;220:507–30. 1038
- [35] McDonald IK, Thornton JM. Satisfying hydrogen bonding poten-  
1022 tial in proteins. *J Mol Biol* 1994;238:777–93. 1039
- [36] Liu S, Zhang C, Zhou H, Zhou Y. A physical reference state  
1023 unifies the structure-derived potential of mean force for  
1024 protein folding and binding. *Proteins* 2004;56:93–101. 1040
- [37] Leahy DJ, Axel R, Hendrickson WA. Crystal structure of  
1025 a soluble form of the human T cell coreceptor CD8 at 2.6 Å  
1026 resolution. *Cell* 1992;68:1145–62. 1041
- [38] Chothia C, Novotny J, Brucoleri R, Karplus M. Domain associ-  
1027 ation in immunoglobulin molecules: the packing of variable  
1028 domains. *J Mol Biol* 1985;186:651–63. 1042
- [39] Colman PM. Structure of antibody–antigen complexes:  
1029 implications for immune recognition. *Adv Immunol* 1988;43:  
99–132. 1043
- [40] Connolly JM, Hansen TH, Ingold AL, Potter TA. Recognition by  
1030 CD8 on cytotoxic T lymphocytes is ablated by several substitu-  
1031 tions in the class I  $\alpha 3$  domain: CD8 and T-cell receptor  
1032 recognize the same class I molecule. *Proc Natl Acad Sci USA*  
1990;87:2137–41. 1044
- [41] Sekimata M, Tanabe M, Sarai A, Yamamoto J, Kariyone A,  
1033 Nakauchi H, et al. Different effects of substitutions at  
1034 residues 224 and 228 of MHC class I on the recognition of  
1035 CD8. *J Immunol* 1993;150:4416–26. 1045
- [42] Quintana FJ, Gerber D, Bloch I, Cohen IR, Shai Y. A structurally  
1036 altered D,L-amino acid TCR $\alpha$  transmembrane peptide  
1037 interacts with the TCR $\alpha$  and inhibits T-cell activation  
1038 in vitro and in an animal model. *Biochemistry* 2007;46:  
2317–25. 1046